

Detecting the Genetic Signatures of Breast Cancer with High-Frequency Ultrasound

Janeese E. Stiles
Department of Biology
Utah Valley University
800 West University Parkway
Orem, Utah 84058 USA

Faculty Advisor: Dr. Timothy E. Doyle

Abstract

Previous studies have shown that high-frequency (HF) ultrasound is sensitive to cell properties such as stiffness and adhesion factors which are a function of protein expression. The goal of this project is to see if HF ultrasound is sensitive enough to detect and differentiate between the five molecular subtypes of breast cancer which are based on protein expression. Since genetic changes precede histological changes in the development of breast cancer, the ability to detect genetic changes (i.e., molecular subtypes) in breast tissue in real time and at the microscopic level will allow surgeons to remove all of the malignant and premalignant tissue during lumpectomies. HF ultrasound personalizes the treatment plan and will be used as a diagnostic technique for precise, image-guided breast cancer surgery. Four breast cancer cell lines with different molecular subtypes and a non-malignant breast cell line will be grown as monolayer cultures. At monolayer confluence, cell and nuclei morphologies of the cell cultures will be determined by phase-contrast microscopy. After microscopy, the monolayers will be ultrasonically tested using a HF ultrasonic test system with a single-element (50 MHz, 6.35-mm) ultrasonic immersion transducer. The resulting ultrasonic waveforms will be analyzed using computational models that simulate the ultrasonic scattering from cells and nuclei as a function of morphology, internal properties, and external properties. The protein expressions associated with the different subtypes will be researched to determine what effects each subtype will have on cell and tissue properties. This method will add a new dimension to pathology and permit more efficient surgical treatment of breast cancer.

Keywords: High-Frequency Ultrasound, Breast Cancer, Molecular Subtype

1. Introduction

In addition to the traditional classifications based on histopathology, breast cancer can be classified by gene expression into five molecular subtypes. These subtypes have been found to be much more predictive of patient prognosis and response to treatment than the traditional classifications. The more aggressive subtypes include the basal-like and Her2+ breast cancers, whereas the least aggressive, most treatable subtype is luminal A breast cancer. Molecular subtypes often show mixed correlation to histopathology, but have a direct connection to the evolution of breast cancer and premalignant lesions.^{1,2} As summarized by Simpson *et al.*,² “The distinct molecular genetic features found in different grades of invasive carcinomas are also mirrored in pre-invasive lesions of comparable morphology.”

The removal of all tumor cells in breast conservation surgery is essential for preventing recurrence of breast cancer. Patients with positive margins have a four times greater risk of local recurrence than those with negative margins.³ An accurate, non-invasive method is therefore needed to provide instant pathology results to the surgeon in the operating room to enable the precise excision of the tumor and surrounding microscopic cancer while saving

as much unaffected tissue as possible. Genetic analyses of margins from oral carcinoma surgery reveal that premalignant changes can be present in histologically normal tissue and can be predictive of oral carcinoma recurrence.^{4,5} Similarly, it has been shown that local recurrence of breast cancer is strongly correlated to molecular subtype.⁶ A technology that could molecularly profile breast tissue rapidly and at high resolution (≤ 1 mm) in margins would therefore be a decidedly useful tool for surgeons and oncologists who wish to reduce local recurrence of the disease in patients, as well as reduce the number of repetitive surgeries required to obtain negative margins.

The objective of this study was to determine if high-frequency (HF) ultrasound (20-100 MHz) can differentiate the molecular subtypes of breast cancer. Previous studies have shown that HF ultrasound can distinguish malignant from normal human epithelial breast cells in cultures, as well as between normal tissue, benign pathologies, ductal carcinomas, and lobular carcinomas in surgical margins.^{7,8} Recently, mutations associated with triple-negative and Her2+ breast cancers have been discovered that are associated with the actin cytoskeleton, integrin signaling, cancer-associated fibroblasts, and extracellular matrix (ECM).^{9,10} These mutations may alter the biomechanical and thus ultrasonic properties of tumor cells. Specifically, biomechanical changes in the cell cytoplasm are hypothesized to arise from triple-negative and Her2+ cancer mutations that code for proteins that regulate the actin cytoskeleton.^{9,11} Such proteins have been measured to have different expression levels between breast cancer subtypes and include thymosin β 4 and β 10 (involved in cytoskeletal binding), keratin type I cytoskeletal 19 (involved in metastatic progression of breast cancer), coactosin-like 1 (regulates actin cytoskeleton), and filamin A, alpha isoform 2 (anchors transmembrane proteins to actin cytoskeleton).¹¹ To test this hypothesis, ultrasonic backscatter spectra from cell cultures were numerically calculated to determine the effect of changes in the biomechanical properties of the cell cytoplasm. Ultrasonic measurements were additionally collected from monolayer cell cultures to determine the feasibility of acquiring corresponding experimental spectra.

2. Methods

2.1. Numerical Studies

Multipole expansions consisting of vector spherical wave functions were used to simulate micro-level ultrasonic scattering from malignant breast cells grown in monolayer cell cultures and with a range of cytoplasm properties. The scattering geometry was configured to represent *in situ* HF ultrasonic pulse-echo measurements of cell cultures grown in polystyrene culture wells (Fig. 1). Cells were modeled as a spherical nucleus surrounded by a spherical cytoplasm shell and embedded in ECM. Figure 2(a) shows a simulated nonconfluent cell monolayer modeled with a close-packed hexagonal packing. Multipole expansions and boundary condition solutions—continuity of stresses and displacements—were used to calculate the ultrasonic waves backscattered from the cell monolayer. Shear and longitudinal wave propagation were simulated as well as mode conversion at the plasma and nuclear membranes. Figure 2(b) is a color plot of the amplitudes of the ultrasonic displacements for the cell monolayer shown in Fig. 2(a). Details of the numerical method are in References 7, 12, and 13. Bulk moduli for the cytoplasm were estimated from ultrasonic wave speed measurements of breast tissue including fatty, glandular, and tumor tissue. Shear moduli for the cytoplasm were estimated from ultrasonic measurements of brain tissue at 1-10 MHz.¹⁴ Note that the shear modulus for tissue increases exponentially with ultrasonic frequency, from 20 kPa at 100 Hz to 300 MPa at 1-10 MHz, where it plateaus to a constant value for higher frequencies.¹⁴ Cell and nuclear diameters were calculated from the mean cellular area (MCA) and mean nuclear area (MNA) of cells from invasive ductal carcinoma without lymph node metastasis.¹⁵

Simulations were performed in the 20-100 MHz range to calculate HF ultrasonic backscatter spectra for the cell monolayer. Frequency dependent attenuation and the response function for a 50-MHz broadband transducer (60-MHz BWHM) were additionally incorporated into the spectra to simulate more realistic measurement conditions in actual breast tissue. In actual experiments, the cell backscatter signals would be convoluted with the specular reflection from the polystyrene well bottom. The application of a signal processing method such as wavelet analysis would therefore be necessary for separating the ultrasonic backscatter from the monolayer and tissue well.⁷

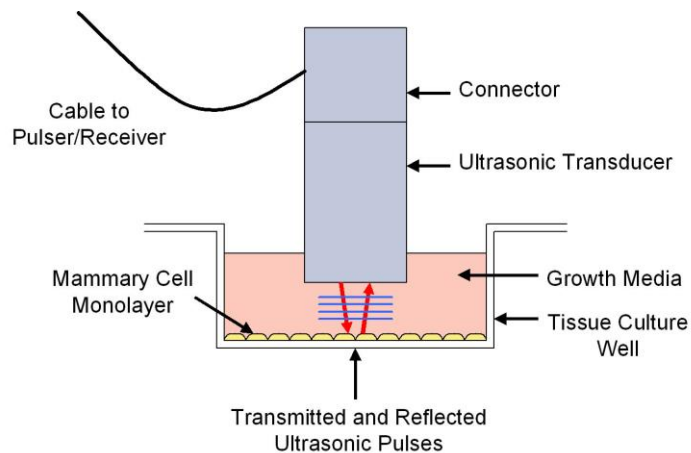


Figure 1. Diagram of simulation and experimental approach. A longitudinal plane wave is incident on a two-dimensional monolayer of nucleated spherical cells. Scattering interactions between the extracellular matrix (ECM), cytoplasm, and nucleus are calculated using multipole expansions and boundary condition solutions.

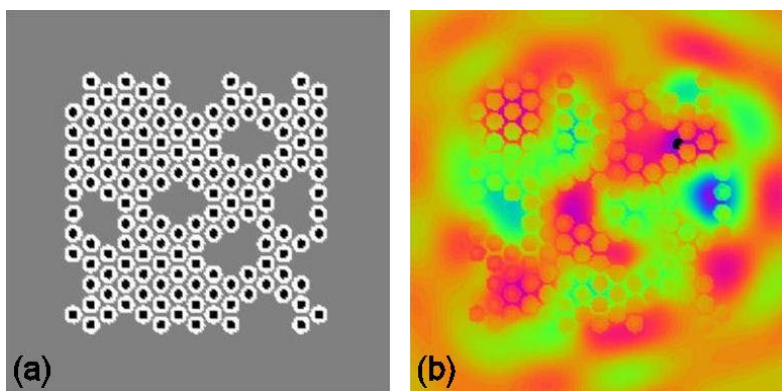


Figure 2. (a) Simulation of a nonconfluent monolayer culture of breast epithelial cells showing cell cytoplasm (white) and nuclei (black). (b) Simulated ultrasonic field amplitudes for the simulated monolayer in (a).

2.2. Cell Culture Studies

Cell lines were selected from a list of 52 widely used breast cancer cell lines for which molecular subtype and other genetic information were provided.¹⁶ Four malignant breast epithelial cell lines and one normal breast epithelial cell line were selected (Table 1). To minimize morphological variations in the cultured cells and enhance molecular and genetic differences, the malignant cell lines were selected from a similar source (primary tumor, ductal carcinomas).¹⁷ The malignant cell lines were grown in a base medium of RPMI-1640 with a final concentration of 10 % fetal bovine serum and 1% penicillin/streptomycin. The normal cell line was grown in a medium consisting of a 1:1 mixture of Dulbecco's modified Eagle's medium and Ham's F12 medium with 0.04 mM Ca⁺⁺; 20 ng/ml epidermal growth factor; 100 ng/ml cholera toxin; 0.01 mg/ml insulin and 500 ng/ml hydrocortisone, 95%; and 5% Chelex-treated horse serum. Cells were cultured at 37.0°C in an atmosphere of 95% air and 5% carbon dioxide.

Initial HF ultrasonic measurements were collected from an HCC70 monolayer culture. The HF ultrasonic system consisted of an ultrasonic immersion transducer (Olympus NDT, V358-SU, 50 MHz, 0.635-cm dia. element), an aluminum test fixture to support the tissue culture well and to position the transducer above the monolayer, a HF square-wave pulser-receiver (UTEX, UT340), a digital oscilloscope (Agilent, DSOX3104A, 1 GHz, 4 analog channels), and a laptop personal computer using LabVIEW for data acquisition. Measurements were acquired using instrument settings and procedures as previously described.⁷

Table 1. Characteristics of selected cell lines. DC = ductal carcinoma.

| Cell Line | Subtype | Phenotype | ER | PR | ERBB2/ HER2 | Source |
|--------------------------|---------|-----------------|----|----|----------------|-------------------|
| HCC38 | Basal B | Triple negative | - | - | - | Primary tumor, DC |
| HCC70 | Basal A | Triple negative | - | - | - | Primary tumor, DC |
| HCC202 | Luminal | ERBB2 amplified | - | - | + | Primary tumor, DC |
| HCC1500 | Luminal | Hormone + | + | + | - | Primary tumor, DC |
| MCF-12F or MCF-10A | | Normal | | | | |

3. Results

3.1. Numerical Results

Frequency spectra calculated for cells having a cytoplasmic shear modulus in the range of 100-300 MPa (Fig. 3) displayed significant changes in spectral shape, including changes in peak locations, amplitudes, and number. The shear modulus range corresponds to an ultrasonic shear wavespeed range of 312-540 m/s. Simulations for a more narrow range of shear moduli (210-250 MPa) showed significantly less change between spectra. The most significant changes in the spectra occur in the 60-100 MHz region [Fig. 3(a)]. Although these changes are significantly reduced when tissue attenuation and the transducer function are included [Fig. 3(b)], a change in the peak frequency of the spectrum is still clearly observed, as well as a change in the shape of the spectrum.

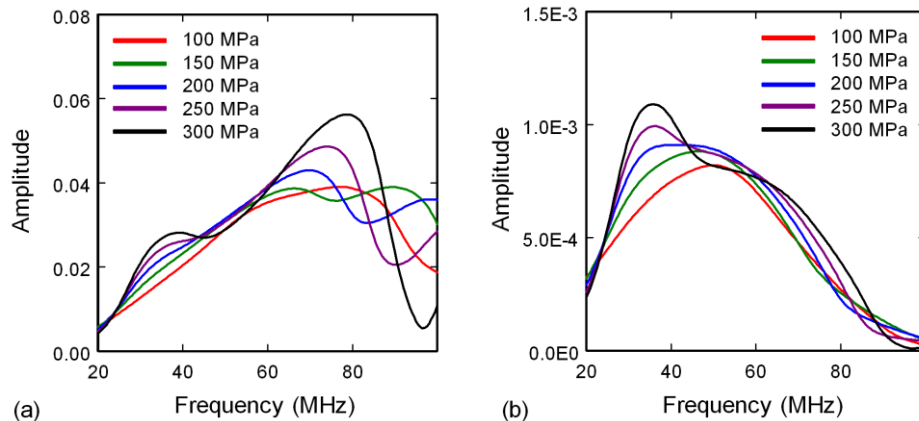


Figure 3. Ultrasonic backscatter spectra of simulated monolayer cell cultures of breast cells with shear moduli in the cytoplasm ranging from 100-300 MPa. (a) Spectra for no tissue attenuation and a flat transducer response. (b) Spectra for frequency dependent tissue attenuation and a broadband 50-MHz transducer.

Frequency spectra for cells having a cytoplasmic bulk modulus in the range of 2.10-2.50 GPa (Fig. 4) displayed changes in peak amplitudes and positions as well. However, in contrast to changes in shear modulus [Fig. 3(a)], an increase in bulk modulus decreased the peak amplitude in the 60-100 MHz region [Fig. 4(a)]. For the attenuation and transducer corrected spectra, the trends are similar to those for changes in shear modulus [Fig. 3(b)], with increasing peak amplitude and decreasing peak frequency with increasing bulk modulus [Fig. 4(b)]. However, the shapes of the peaks for the shear and bulk modulus changes are different for shear moduli above 200 MPa and bulk

moduli above 2.3 GPa. The simulated bulk modulus range spans from the softest breast tissue (fat tissue at 2.10 GPa) with a longitudinal wavespeed of 1430 m/s, to the stiffest breast tissue (tumor tissue at 2.50 GPa) with a longitudinal wavespeed of 1560 m/s.

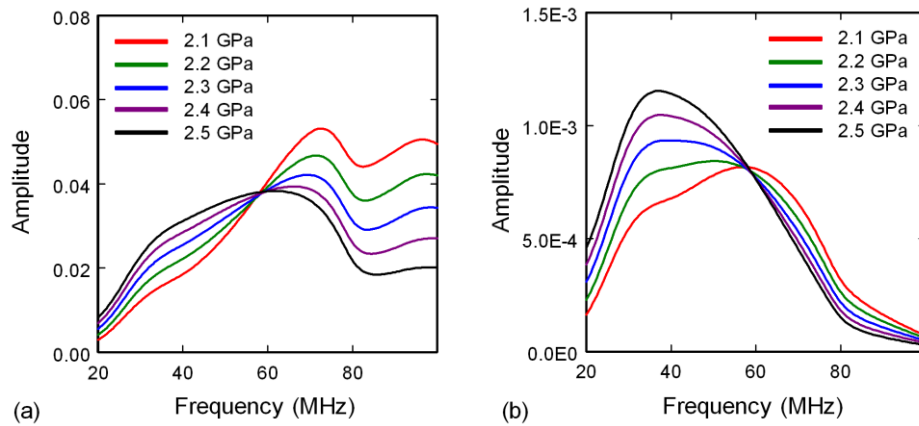


Figure 4. Ultrasonic backscatter spectra of simulated monolayer cell cultures of breast cells with bulk moduli in the cytoplasm ranging from 2.10-2.50 GPa. (a) Spectra for no tissue attenuation and a flat transducer response. (b) Spectra for frequency dependent tissue attenuation and a broadband 50-MHz transducer.

Breast epithelial cell size increases for pathologies such as atypical ductal hyperplasia and invasive ductal carcinoma.¹⁵ Because previous work had shown that changes in cell size can also affect the structure of HF ultrasonic spectra,⁷ simulations were performed for monolayers of breast cells having diameters ranging from 14-22 μm . Since the nuclei in hyperplastic and malignant cells also typically increase in size, the simulations accounted for this by increasing the nucleus size in proportion to the cell size. The results (Fig. 5) show that increasing the cell and nucleus size decreases the frequency of the primary spectral peak. These results have been verified by previous experimental data.⁷ However, the spectral changes resulting from cell size variation are significantly different from those resulting from changes in either the shear or bulk moduli. Consequently, size changes result in greater spectral shape changes, particularly in frequencies greater than 50 MHz.

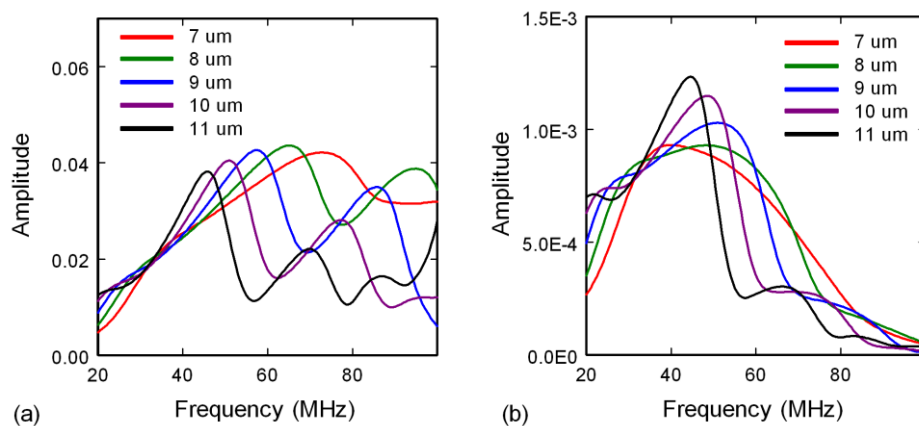


Figure 5. Ultrasonic backscatter spectra of simulated monolayer cell cultures of breast cells with cell radius ranging from 7.0-11.0 μm . Nuclear radius is half the cell radius. (a) Spectra for no tissue attenuation and a flat transducer response. (b) Spectra for frequency dependent tissue attenuation and a broadband 50-MHz transducer.

3.2. Initial Test Results With Cell Cultures

Figure 6 displays representative results from ultrasonic testing of initial monolayer cultures of the HCC70 and HCC202 cell lines. The cells were seeded at concentrations of 5×10^5 cells/ml (HCC70) and 2×10^5 cells/ml (HCC202) in 6-well culture plates. Control wells with growth media only were also tested. The pulse-echo signals from the control wells contained solely the reflection from the polystyrene well bottom. The pulse-echo signals from wells seeded with the malignant cell lines were also dominated by the well bottom reflection, but also contained weak reflections in front (earlier in time) of the well reflection. These weak reflections can be ascribed to the malignant breast cancer cell monolayers due to their position in the signal immediately preceding the well reflection and their presence only in the seeded well plates. The spectra of monolayer reflections from the same cell line but from different wells were reproducible, showing the same peak position and width [Fig. 6(a) and (b)]. However, the spectra between cell lines were significantly different, with obvious differences in peak position and shape [Fig. 6(c)].

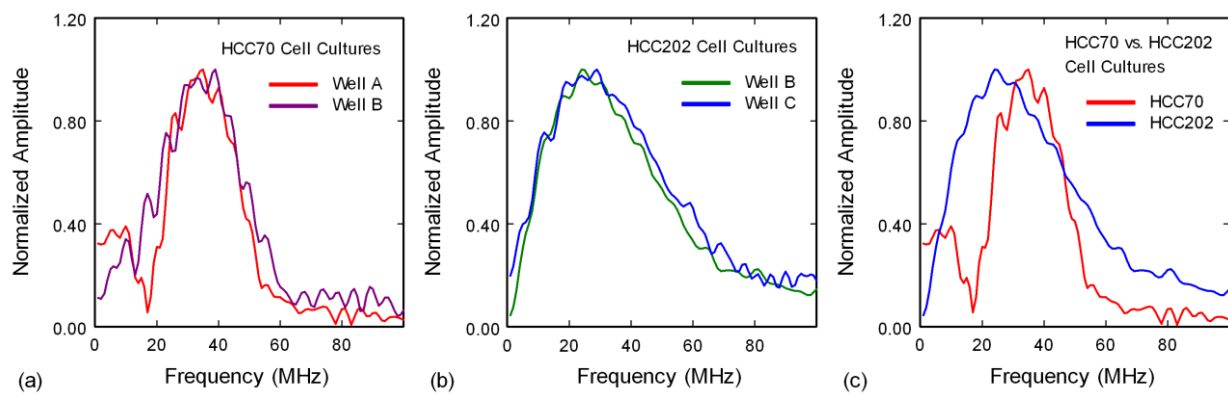


Figure 6. (a) Ultrasonic pulse-echo spectra from two different wells of HCC70 cell cultures. (b) Ultrasonic pulse-echo spectra from two different wells of HCC202 cell cultures. (c) Comparison of HCC70 and HCC202 spectra, exhibiting differences in peak position and peak width due to different intracellular biomechanical properties.

4. Discussion

The simulation results indicate that both cytoplasmic shear and bulk modulus have a significant effect on HF ultrasonic backscatter spectra. The most significant differences between the shear and bulk moduli spectra occur at frequencies above 60 MHz [Figs. 3(a) and 4(a)]. Tissue attenuation and transducer response, however, suppress these differences but still produce spectra with subtle changes in peak shape [Figs. 3(b) and 4(b)]. Changes in cell and nucleus size are also strong at frequencies above 60 MHz [Fig. 5(a)], but high-frequency suppression results in greater spectral shape changes than are observed for changes in shear and bulk moduli.

In order to determine differences in cytoplasmic material properties in malignant breast cells, and therefore differences in cytoplasmic proteins and cytoskeletal structure, numerical results such as those presented could be expanded and used to simultaneously determine cytoplasmic bulk and shear modulus. It may be additionally possible to determine cell and nucleus size. The presented numerical spectra indicate that each of the parameters modeled—cytoplasmic shear modulus, cytoplasmic bulk modulus, cell size and nucleus size—has a unique effect on the spectral structure. With sufficient model and experimental spectra, a method such as principal component analysis could be used to analyze the spectra of breast cancer cells and determine their properties. In turn, these properties should correlate to molecular subtype or specific mutations that affect cytoskeletal proteins.

Since the greatest changes in the simulated spectra occur in the 60-100 MHz region, methods that would enhance the signal from these frequencies would optimize the ability to determine cytoplasmic moduli and cell/nucleus size. Such methods include the use of higher frequency transducers or data analysis techniques that remove tissue attenuation and transducer response effects from experimental spectra. Neglecting tissue attenuation, a broadband ultrasonic transducer with a center frequency of 80 MHz would theoretically produce spectra similar to those in

Figs. 3(a), 4(a), and 5(a). Additionally, once the response of the transducer and the attenuation of the tissue have been characterized, it should be possible to subtract these effects from the experimental spectra and enhance the 60-100 MHz band.

The initial experimental results as shown in Fig. 6 showed waveform signals that can be positively attributed to different cell lines. Spectra from the waveforms, Fig. 6, displayed different peak characteristics including maximum peak position and peak width. Additionally, the time-domain waveforms displayed different peak densities between the two cell lines, including multiple peaks for the HCC70 cell line. Since HCC70 is from a triple-negative molecular subtype and HCC202 is from a luminal molecular subtype, the initial results support the hypothesis of this project that HF ultrasound is sensitive enough to detect and differentiate between molecular subtypes of breast cancer.

5. Conclusions

Initial numerical simulations indicate that two principal biomechanical properties of breast cells, the shear and bulk moduli of the cytoplasm, significantly affect HF ultrasonic backscatter spectra. Although cell and nucleus size also significantly affect the backscatter spectra, the spectral changes due to size changes differ from those of changes in the moduli. A feature classification approach such as principal component analysis may therefore be valuable for separating cytoplasm properties from cell morphology. From a biomolecular perspective, mutations in the more aggressive subtypes of breast cancer have been discovered that are associated with the proteins responsible for the maintenance of the actin cytoskeleton. Since the cytoplasm properties are strongly influenced by the actin cytoskeleton, the potential exists for establishing a mechanistic link between HF ultrasound and specific genetic mutations in the molecular subtypes of breast cancer. Initial experiments have shown that waveform signals can be obtained from monolayer cultures of malignant breast cells. Spectra from these initial waveforms are able to differentiate between cell lines having different molecular subtypes, thereby supporting the hypothesis of this research.

6. Acknowledgments

We gratefully thank Leigh Neumayer, Rachel Factor, Bryan Welm, Alana Welm, and our other colleagues in the Breast Disease-Oriented Team (BDOT) at the Huntsman Cancer Institute for their continuing support, assistance, and advice. We also thank Brent Barger and Sam Rushforth at Utah Valley University for their support of this research. This project was funded by a Utah Valley University Presidential Fellowship Award.

7. References

1. J. D. Wulfkühle, D. C. Sgroi, H. Krutzsch, K. McLean, K. McGarvey, M. Knowlton, S. Chen, H. Shu, A. Sahin, R. Kurek, D. Wallwiener, M. J. Merino, E. F. Petricoin, III, Y. Zhao, and P. S. Steeg, "Proteomics of human breast ductal carcinoma *in situ*," *Cancer Research* **62**, 6740-6749 (2002).
2. P. T. Simpson, J. S. Reis-Filho, T. Gale, and S. R. Lakhani, "Molecular evolution of breast cancer," *Journal of Pathology* **205**, 248-254 (2005).
3. S. E. Singletary, "Surgical margins in patients with early-stage breast cancer treated with breast conservation therapy," *American Journal of Surgery* **184**, 383-393 (2002).
4. P. G. van der Toom, J. A. Veltman, F. J. Bot, J. M. A. de Jong, J. J. Manni, F. C. S. Ramaekers, and A. H. N. Hopman, "Mapping of resection margins of oral cancer for p53 overexpression and chromosome instability to detect residual (pre)malignant cells," *Journal of Pathology* **193**, 66-72 (2001).
5. P. P. Reis, L. Waldron, B. Perez-Ordóñez, M. Pintilie, N. Naranjo Galloni, Y. Xuan, N. K. Cervigne, G. C. Warner, A. A. Makitie, C. Simpson, D. Goldstein, D. Brown, R. Gilbert, P. Gullane, J. Irish, I. Jurisica, and S. Kamel-Reid, "A gene signature in histologically normal surgical margins is predictive of oral carcinoma recurrence," *BMC Cancer* **11**, 437 (2011).
6. K. D. Voduc, M. C. U. Cheang, S. Tyldesley, K. Gelmon, T. O. Nielsen, and H. Kennecke, "Breast cancer subtypes and the risk of local and regional relapse," *Journal of Clinical Oncology* **28**, 1684-1691 (2010).

7. T. E. Doyle, H. Patel, J. B. Goodrich, S. Kwon, B. J. Ambrose, and L. H. Pearson, "Ultrasonic differentiation of normal versus malignant breast epithelial cells in monolayer cultures," *J. Acoust. Soc. Am.* **128**, EL229-EL235 (2010).
8. T. E. Doyle, R. E. Factor, C. L. Ellefson, K. M. Sorensen, B. J. Ambrose, J. B. Goodrich, V. P. Hart, S. C. Jensen, H. Patel, and L. A. Neumayer, "High-frequency ultrasound for intraoperative margin assessments in breast conservation surgery: a feasibility study," *BMC Cancer* **11**, 444 (2011).
9. S. P. Shah, A. Roth, R. Goya, A. Oloumi, G. Ha, Y. Zhao, G. Turashvili, J. Ding, K. Tse, G. Haffari, A. Bashashati, L. M. Prentice, J. Khattra, A. Burleigh, D. Yap, V. Bernard, A. McPherson, K. Shumansky, A. Crisan, R. Giuliani, A. Heravi-Moussavi, J. Rosner, D. Lai, I. Birol, R. Varhol, A. Tam, N. Dhalla, T. Zeng, K. Ma, S. K. Chan, M. Griffith, A. Moradian, S.-W. G. Cheng, G. B. Morin, P. Watson, K. Gelmon, S. Chia, S.-F. Chin, C. Curtis, O. M. Rueda, P. D. Pharoah, S. Damaraju, J. Mackey, K. Hoon, T. Harkins, V. Tadigotla, M. Sigaroudinia, P. Gascard, T. Tlsty, J. F. Costello, I. M. Meyer, C. J. Eaves, W. W. Wasserman, S. Jones, D. Huntsman, M. Hirst, C. Caldas, M. A. Marra, and S. Aparicio, "The clonal and mutational evolution spectrum of primary triple-negative breast cancers," *Nature* **486**, 395-399 (2012).
10. J. Tchou, A. V Kossenkov, L. Chang, C. Satija, M. Herlyn, L. C. Showe, and E. Puré, "Human breast cancer associated fibroblasts exhibit subtype specific gene expression profiles," *BMC Medical Genomics* **5**, 39 (2012).
11. J. He, S. A. Whelan, M. Lu, D. Shen, D. U. Chung, R. E. Saxton, K. F. Faull, J. P. Whitelegge, and H. R. Chang, "Proteomic-based biosignatures in breast cancer classification and prediction of therapeutic response," *International Journal of Proteomics* **2011**, Article ID 896476 (2011).
12. T. E. Doyle, K. H. Warnick, and B. L. Carruth, "Histology-based simulations for the ultrasonic detection of microscopic cancer *in vivo*," *J. Acoust. Soc. Am.* **122**, EL210-EL216 (2007).
13. T. E. Doyle, A. T. Tew, K. H. Warnick, and B. L. Carruth, "Simulation of elastic wave scattering in cells and tissues at the microscopic cancer level," *J. Acoust. Soc. Am.* **125**, 1751-1767 (2009).
14. S. A. Lippert and M. J. Grimm, "Estimating the material properties of brain tissue at impact frequencies: A curve fitting solution," *2003 Summer Bioengineering Conference*. Key Biscayne, Florida (June 25-29, 2003).
15. B. Arora, Renu, A. C. Kakade, and B. Rekhi, "Diagnostic application of mean nuclear area (MNA) measured by computerized interactive morphometry in breast cancer," *The Internet Journal of Pathology* **5**, 1-13 (2007).
16. J. Kao, K. Salari, M. Bocanegra, Y.-L. Choi, L. Girard, J. Gandhi, K. A. Kwei, T. Hernandez-Boussard, P. Wang, A. F. Gazdar, J. D. Minna, and J. R. Pollack, "Molecular Profiling of Breast Cancer Cell Lines Defines Relevant Tumor Models and Provides a Resource for Cancer Gene Discovery," *PLoS ONE* **4**, e6146 (2009).
17. A. F. Gazdar, V. Kurvari, A. Virmani, L. Gollahon, M. Sakaguchi, M. Westerfield, D. Kodagoda, V. Stasny, H. T. Cunningham, I. I. Wistuba, G. Tomlinson, V. Tonk, R. Ashfaq, A. M. Leitch, J. D. Minna, and J. W. Shay, "Characterization of paired tumor and non-tumor cell lines established from patients with breast cancer," *Int. J. Cancer* **78**, 766-774 (1998).